

# Leptonic scalar portal: Origin of muon $g - 2$ anomaly and dark matter?

S. N. Gninenko<sup>1</sup> and N. V. Krasnikov<sup>1,2</sup>

<sup>1</sup>*Institute for Nuclear Research, 117312 Moscow, Russia*

<sup>2</sup>*Joint Institute for Nuclear Research, 141980 Dubna, Russia*

(Dated: July 8, 2022)

We present a model explaining both the  $4.2\sigma$  muon  $g - 2$  anomaly and the relic density of dark matter (DM) in which DM interacts with the Standard Model (SM) via a scalar portal boson  $\varphi$  carrying both dark and SM leptonic numbers, and mediating a nondiagonal interaction between the electron and muon that allows  $e \leftrightarrow \mu$  transitions. The  $\varphi$  could be produced in high-energy electron scattering off a target nuclei in the reaction  $eZ \rightarrow \mu Z \varphi$  followed by the prompt invisible decay  $\varphi \rightarrow$  DM particles and searched for in events with large missing energy accompanied by a single outgoing muon in the final state. Interestingly, several events with a similar signature have been observed in a data sample of  $\simeq 3 \times 10^{11}$  electrons on target collected during 2016-2018 for the search for light dark matter in the NA64 experiment at the CERN SPS [PRL **123**, 121801 (2019)]. Attributing so far these events to background allows us to set first constraints on the  $\varphi$  mass and couplings while leaving at the same time decisively probing the origin of these events and a large fraction of the remaining parameter space to a near exiting future with the upgraded NA64 detector or other planned experiments.

PACS numbers:

The recent precise determination of the anomalous magnetic moment of the positive muon  $a_\mu = (g - 2)_\mu/2$  from the experiment E989 at FNAL [1] confirmed the previous measurements of Ref.[2], and gives result which is about  $4.2\sigma$  higher than the Standard Model (SM) prediction, see, e.g., [3–14]

$$a_\mu^{exp} - a_\mu^{SM} = (251 \pm 59) \times 10^{-11} \quad (1)$$

This result may signal the existence of new physics (NP) below the electroweak scale ( $\ll 100$  GeV), see e.g., Ref.[15]. For example, one of the most attractive explanations of the anomaly suggests the existence of a sub-GeV gauge boson, which can be probed in a near future at a fixed-target experiment, see e.g. [16–26].

Another motivation for searches of NP in the low-mass range come from the dark matter (DM) sector. Despite many intensive searches at the accelerator and in non-accelerator experiments, still little is known about the origin and dynamics of the dark sector itself. One difficulty so far is that DM can be probed only through its gravitational interaction. Thus, sensitive searches for possible portals that could transmit new feeble interaction between the ordinary and dark matter are crucial and, indeed, they have received significant attention in recent years [27–31].

The goal of this work is to show that both the  $4.2\sigma$  muon  $g - 2$  anomaly and the relic density of dark matter (DM) could be explained by a model in which DM interacts with the Standard Model (SM) via a scalar portal boson  $\varphi$  carrying SM  $L_e$  and  $L_\mu$  leptonic numbers. The  $\varphi$  mediates a nondiagonal interaction between the electron and muon that allows  $e \leftrightarrow \mu$  transitions, while the leptonic numbers are conserved. Similar models were considered in the recent past, but unlike the present model they considered diagonal interactions transmitted by a mediator carrying different quantum numbers, see, e.g.

Ref. [32–36]. It is assumed that the  $\varphi$  decays predominantly invisibly,  $\Gamma(\varphi \rightarrow \text{invisible})/\Gamma_{tot} \simeq 1$ , e.g., into dark sector particles, thus escaping stringent constraints placed today on the visible decay modes of the  $\varphi$  into SM particles from collider, fixed-target, and atomic experiments [37]. The most stringent limits on the invisible  $\varphi$  in the sub-GeV mass range are obtained, so far, for the case of scalars  $\varphi$  coupled to electron and muon by the low-energy experiments searching for the muon decay  $\mu \rightarrow e\varphi$  [37], leaving a large area of the parameter space for the leptonic  $\varphi$  still unexplored. Therefore in the following we assume that  $m_\varphi \gtrsim m_\mu$ .

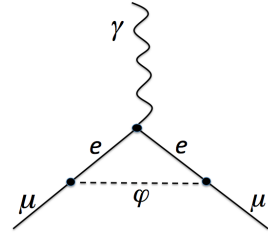


FIG. 1: One-loop contribution of the leptonic scalar  $\varphi$  to  $\Delta a_\mu$ .

Consider the interaction of a complex scalar mediator  $\varphi(x)$  with electrons and muons, namely

$$L_{\varphi\mu e} = -h_{\mu e} \bar{e}_L \mu_R \varphi + H.c., \quad (2)$$

where  $e_L = (\frac{1-\gamma_5}{2})e$ ,  $\mu_R = (\frac{1+\gamma_5}{2})\mu$ . The interaction (2) is invariant under the  $L_e$ ,  $L_\mu$  flavor global transformations  $\varphi(x) \rightarrow \exp(i\alpha_e + i\alpha_\mu)\varphi(x)$ ,  $\mu(x) \rightarrow \exp(-i\alpha_\mu)\mu(x)$ , and  $e(x) \rightarrow \exp(i\alpha_e)e(x)$ . Due to the postulated global symmetry, the Lagrangian (2) contains only nondiagonal terms like  $-h_{\mu e} \bar{e}_L \mu_R$ , and flavor diagonal terms  $-h_{ee} \bar{e}e\varphi$  and  $-h_{\mu\mu} \bar{\mu}\mu\varphi$  are prohibited. As a consequence, for massless neutrino the interaction (2)

transmitted by the leptonic  $\varphi$  conserves both muon and electron lepton numbers. The interaction (2) leads to additional contributions to the electron and muon ( $g-2$ ). One-loop contribution to  $a_\mu$  is shown in Fig. and it reads [38]

$$\Delta a_\mu = \frac{h_{\mu e}^2}{16\pi^2} \frac{m_\mu^2}{m_\varphi^2} L, \quad (3)$$

$$L = \frac{1}{2} \int_0^1 dx \frac{2x^2(1-x)}{(1-x)(1-\lambda^2 x) + (\epsilon\lambda)^2 x}, \quad (4)$$

where  $\epsilon = \frac{m_e}{m_\mu}$  and  $\lambda = \frac{m_\mu}{m_\varphi}$ . For electron magnetic moment we must replace  $m_\mu$  to  $m_e$  and  $m_e$  to  $m_\mu$  in formulas (3), (4). For  $m_\varphi \gg m_\mu$  one can find [38] that

$$\Delta a_{e(\mu)} = \frac{h_{\mu e}^2}{48\pi^2} \frac{m_{e(\mu)}^2}{m_\varphi^2}, \quad (5)$$

and  $\frac{\Delta a_e}{\Delta a_\mu} = \left(\frac{m_e}{m_\mu}\right)^2$ . If we assume that the additional interaction explains the muon anomaly (1), then

$$h_{\mu e} = (1.1 \pm 0.1) \times 10^{-3} \left(\frac{m_\varphi}{m_\mu}\right). \quad (6)$$

for  $m_\varphi \gg m_\mu$ . As it was mentioned previously in the rest of the paper we assume that  $m_\varphi > m_\mu$ . This assumption allows us to prohibit the decay  $\mu \rightarrow e\varphi$  for which experimental data restrict rather strongly the coupling constant  $h_{\mu e}$ . For our estimates we shall use the conventional point  $m_\varphi = 3m_\mu$  resulting in

$$h_{\mu e} = (3.3 \pm 0.3) \times 10^{-3}. \quad (7)$$

for explaining the value (1).

The  $SU_L(2) \otimes U(1)$  invariant generalization of the interaction (2) is

$$L_{\mu e, gen} = -\frac{h_1 h_2}{M} (\bar{\nu}_e, \bar{e})_L H \varphi \mu_R + H.c., \quad (8)$$

where  $\frac{h_1 h_2 \langle H \rangle}{M} = h_{\mu e}$ , and  $\langle H \rangle = 174 \text{ GeV}$  is the vacuum expectation value of the Higgs isodoublet  $H$ . In the unitary gauge  $H = (0, \frac{h}{\sqrt{2}} + \langle H \rangle)$ , where  $h$  is the Higgs field. Note that the complex scalar mediator  $\varphi(x)$  is a singlet under the  $SU_c(3) \otimes SU_L(2) \otimes U(1)$  SM gauge group. Due to possible interaction  $L = -\lambda_{H\phi} H^+ H \varphi^* \varphi$  of the scalar  $\varphi$  with the Higgs isodoublet, Higgs boson would decay invisibly into a  $\varphi$  pair,  $h \rightarrow \varphi\varphi^*$ , with a rate given by  $\Gamma(h \rightarrow \varphi\varphi^*) = \frac{\lambda_{H\phi}^2 v^2}{16\pi m_h} (1 - \frac{4m_\varphi^2}{m_h^2})^{1/2}$  assuming that the invisible decay  $\varphi \rightarrow DM \text{ particles}$  is dominant (see below). Here  $m_h$  is the Higgs boson mass and  $v = 246 \text{ GeV}$ . From the existing bounds on the Higgs boson invisible decay width [37] one can obtain an upper bound on the coupling constant  $\lambda_{H\phi} \leq 0.01$ . The interaction (8) is nonrenormalizable and it conserves both  $L_e$  and  $L_\mu$  flavor numbers in the approximation of massless

neutrino. One can obtain the effective nonrenormalizable interaction (8) from the renormalizable interaction with vectorlike fermion  $E$ , namely

$$L_{ER\mu e} = -(h_1(\bar{\nu}_e, \bar{e})_L H E_R + h_2 \bar{E}_L \mu_R \varphi + H.c.) - M \bar{E} E \quad (9)$$

Suppose the  $\varphi$ -boson interacts with dark matter particles. Several models can be considered. First, the  $\varphi(x)$  field could have interaction with two dark matter complex scalars  $s_1(x)$  and  $s_2(x)$  given by

$$L_{\varphi s_1 s_2} = g_{\varphi s_1 s_2} \varphi s_1 s_2 + H.c. \quad (10)$$

Note that the coupling constant  $g_{\varphi s_1 s_2}$  has the dimension of the mass. The interaction (10) is invariant under global transformations  $\varphi \rightarrow \exp(i\alpha_1 + i\alpha_2)\varphi$ , and  $s_i \rightarrow \exp(-i\alpha_i)s_i$ , with  $i = 1, 2$ . As a consequence in the approximation of massless neutrino both  $L_e$  and  $L_\mu$  lepton flavors are conserved.

Consider another model, when the scalar  $\varphi$  interacts with two light dark matter fermions  $\psi_1$  and  $\psi_2$  with the Lagrangian

$$L_{\varphi\psi_1\psi_2} = g_{\varphi\psi_1\psi_2} \varphi \bar{\psi}_1 \psi_2 + H.c. \quad (11)$$

Again interaction (11) conserves both  $L_e$  and  $L_\mu$  lepton flavors. For the Lagrangians (10) and (11) the  $\varphi$  decay rate into  $s_1, s_2$  and  $\psi_1, \psi_2$  DM particles is

$$\Gamma(\varphi \rightarrow s_1 s_2) = \frac{g_{\varphi s_1 s_2}^2}{8\pi} \frac{p_1}{m_\varphi^2}, \quad (12)$$

and

$$\Gamma(\varphi \rightarrow \psi_1 \psi_2) = \frac{g_{\varphi\psi_1\psi_2}^2 p_1}{4\pi} \left(1 - \frac{(m_1 + m_2)^2}{m_\varphi^2}\right) \quad (13)$$

respectively, and  $p_1 = \frac{[(m_\varphi^2 - (m_1 + m_2)^2)(m_\varphi^2 - (m_1 - m_2)^2)]^{1/2}}{2m_\varphi}$  is the momentum of the particle 1 in the rest frame of the  $\varphi$ , and  $m_1$  and  $m_2$  are the masses of particles 1 and 2. Here, we assume that  $m_\varphi > m_1 + m_2$ . The decay width of  $\varphi$  into  $\mu^+ e^-$  is given by

$$\Gamma(\varphi \rightarrow \mu^+ e^-) = \frac{h_{\mu e}^2 p_e}{8\pi} \left(1 - \frac{m_e^2 + m_\mu^2}{m_\varphi^2}\right), \quad (14)$$

where  $p_e$  is the electron momentum in the center of mass frame. The annihilation cross sections of  $s_1, s_2$  into  $\mu e$  pair in the nonrelativistic approximation in  $s$ -wave is

$$\begin{aligned} \sigma_{an}(s_1 s_2 \rightarrow e^+ \mu^-) v_{rel} &= \sigma_{an}(s_1 s_2 \rightarrow e^- \mu^+) v_{rel} \\ &= |M|_1^2 \frac{p_{ecm}}{16\pi(m_1 + m_2)m_1 m_2} \end{aligned} \quad (15)$$

where

$$|M|_1^2 = g_{\varphi s_1 s_2}^2 h_{\mu e}^2 \frac{((m_1 + m_2)^2 - m_e^2 - m_\mu^2)}{(m_\varphi^2 - (m_1 + m_2)^2)^2} \quad (16)$$

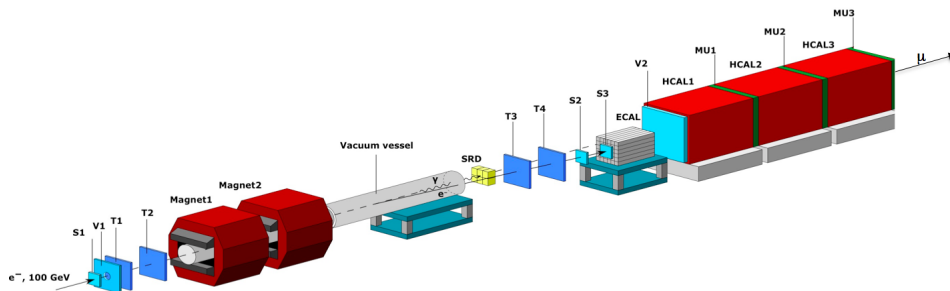


FIG. 2: Schematic illustration of the setup to search for the  $\varphi \rightarrow invisible$  decay of the leptonic scalar  $\varphi$  produced in the reaction  $eZ \rightarrow \mu Z \varphi$  of 100 GeV  $e^-$ 's incident on the active ECAL target of the NA64e experiment.

and  $p_{ecm}$  is the momentum of electron in the center of mass frame[59] For the simplest case of dark matter particles with equal masses,  $m_1 = m_2 \gg m_\mu$ , the annihilation cross section is

$$\sigma_{an}(s_1 s_2 \rightarrow e^+ \mu^-) v_{rel} = \frac{h_{\mu e}^2 g_\varphi^2 s_1 s_2}{8\pi(m_\varphi^2 - 4m_1^2)^2} \quad (17)$$

The treatment of general case with nonequal masses is straightforward and does not qualitatively changes our main conclusions. For fermions  $\psi_1, \psi_2$  in the non-relativistic approximation the annihilation cross section  $\sigma_{an}(\psi_1 \psi_2 \rightarrow e^- \mu^+) v_{rel}$  is given by the formula (15) where

$$|M|_2^2 = \frac{g_\varphi^2 \psi_1 \psi_2}{2} h_{\mu e}^2 \frac{1}{(m_\varphi^2 - (m_1 + m_2)^2)^2} \times ((m_1 + m_2)^2 - m_e^2 - m_\mu^2) m_1 m_2 v_{rel}^2 \quad (18)$$

The total annihilation cross section is given by

$$\sigma_{an,tot} v_{rel} = \frac{h_{\mu e}^2 g_\varphi^2 \psi_1 \psi_2 m_1^2 v_{rel}^2}{8\pi(m_\varphi^2 - 4m_1^2)^2}, \quad (19)$$

where  $\sigma_{an,tot} = \sigma_{an}(\psi_1 \psi_2 \rightarrow e^- \mu^+) + \sigma_{an}(\psi_1 \psi_2 \rightarrow e^+ \mu^-)$ . Thus, we see that in the nonrelativistic limit model with scalar DM particles has  $s$ -wave behavior that contradicts to the Planck data [39][60]

For the model with fermionic DM, we have  $p$ -wave behavior for the annihilation cross section that allows us to escape Planck restrictions [39]. We assume that at the early Universe light DM is in equilibrium with ordinary matter. From the requirement that the relic density of DM is explained by the model, we can estimate the coupling constant  $g_\varphi \psi_1 \psi_2$  using standard formulae for calculations of the DM density [40–44]. For this estimate we assume that the  $p$ -wave annihilation cross section  $\langle \sigma_{an} v_{rel} \rangle = O(1) pb$ , and the average relative velocity of annihilating DM particles  $\langle v_{rel} \rangle \sim c/3$  which corresponds to the observed DM density of the Universe [45]. Consider the simplest example with  $m_1 = m_2 \gg m_\mu$ . As a consequence of the formula (19) we find that

$$\frac{h_{\mu e}^2 g_\varphi^2 \psi_1 \psi_2 m_1^2}{4\pi(m_\varphi^2 - (m_1 + m_2)^2)^2} = O(10 pb) \quad (20)$$

For the case  $m_\varphi = 3m_1$  we find

$$h_{\mu e} g_\varphi \psi_1 \psi_2 \sim 10^{-3} \left( \frac{m_\varphi}{GeV} \right) \quad (21)$$

In the assumption that the model explains muon  $g-2$  we find that  $g_\varphi \psi_1 \psi_2 \sim 0.1$  and it depends rather weakly on the  $\varphi$  mass. As a consequence we obtain that  $g_\varphi \psi_1 \psi_2 \geq h_{\mu e}$  for  $m_\varphi \leq 10 GeV$  and the mediator  $\varphi$  decays mainly invisibly into DM particles. So we find that our model can explain both the  $(g-2)_\mu$  anomaly and the dark matter relic abundance.

Let us briefly discuss constraints on the model from the existing data. Note, that as both  $L_e$  and  $L_\mu$  lepton numbers are conserved the muonium to antimuonium conversion,  $\mu^+ e^- \rightarrow \mu^- e^+$ , is prohibited. As we already mentioned, assuming the invisible  $\varphi$  boson decay is predominant, i.e.  $\Gamma(\varphi \rightarrow all) \simeq \Gamma(\varphi \rightarrow DM)$ , the constraints on coupling  $h_{\mu e}$  from Higgs boson decays are quite modest. The interaction (2) would also result in LFV-like semivisible  $Z$ -boson decays  $Z \rightarrow e^\pm e^\mp \rightarrow e^\pm \mu^\mp \varphi$ ;  $\varphi \rightarrow invisible$  and  $Z \rightarrow \mu^\pm \mu^\mp \rightarrow \mu^\pm e^\mp \varphi$ ;  $\varphi \rightarrow invisible$ . For  $m_\varphi \ll m_Z$  the branching ratio  $\frac{\Gamma(Z \rightarrow \mu^\pm e^\mp \varphi)}{\Gamma(Z \rightarrow e^+ e^-)} \sim \frac{h_{\mu e}^2}{4\pi^2}$ . Assuming  $m_\varphi = 3m_\mu$  and  $h_{\mu e} = 3.3 \times 10^{-3}$ , one gets  $\frac{\Gamma(Z \rightarrow \mu^\pm e^\mp \varphi)}{\Gamma(Z \rightarrow all)} \sim 10^{-8}$ . This can be compared with the best experimental constraint  $\frac{\Gamma(Z \rightarrow \mu^\pm e^\mp)}{\Gamma(Z \rightarrow all)} < 7.5 \times 10^{-7}$  [37] which is much weaker. Assuming that for the missing mass  $\Delta m_{miss} \lesssim 5 GeV$ , which is the experimental resolution of the  $Z$ -mass peak [46], the decays  $Z \rightarrow e^\pm \mu^\mp \varphi$  and  $Z \rightarrow e^\pm \mu^\mp$  are indistinguishable, one could get  $h_{\mu e} \lesssim 3 \times 10^{-2}$  for the sub-GeV  $m_\varphi$  region. Our model also predicts the  $K \rightarrow \mu \nu \rightarrow e \nu \varphi$  decay chain with the branching ratio  $Br(K \rightarrow e \nu \varphi) \sim O\left(\frac{h_{\mu e}^2}{8\pi^2}\right) \sim 2 \times 10^{-7}$ . By using the experimental constraints  $Br(K \rightarrow e \nu \bar{\nu}) < 6 \times 10^{-5}$  for the momentum range 220-230 MeV/c [47] and a phase-space spectrum for the  $K \rightarrow e \nu \varphi$  decay one can obtain modest bounds  $h_{\mu e} \lesssim 7 \times 10^{-2}$  for the mass range  $m_\varphi \lesssim 200 MeV$ . For  $m_K - m_\varphi \gtrsim 250 MeV$  bound from  $K \rightarrow e \nu \varphi$  decay does not work due to kinematics constraints of Ref.[47].

The stronger limits on coupling  $h_{\mu e}$  comes from anomalous magnetic moment of muon. By using Eq.(1) we obtain that at  $3\sigma$  level the contribution of new physics

to  $(g-2)_\mu$  is  $\Delta a_\mu = a_\mu^{exp} - a_\mu^{SM} \lesssim 428 \times 10^{-11}$ . Using Eqs.(3 - 5) one gets for  $m_\varphi > m_\mu$ , that  $h_{\mu e} \lesssim 1.42 \times 10^{-3} (\frac{m_\varphi}{m_\mu})$  at  $3\sigma$  level. For  $m_\varphi = 3m_\mu$  we find that  $h_{\mu e} \leq 4.26 \times 10^{-3}$ . Note that bound from  $\Delta a_\mu$  gets weaker proportionally to  $m_\varphi$ , and for large masses  $m_\varphi \gtrsim$  a few GeV the ATLAS bound from the  $Z$ -decays becomes stronger.

Additional constraints can be obtained from the NA64e experiment. For the sensitivity estimate we will use NA64e results on the search for light DM production in invisible decays of dark-photon ( $A'$ ) mediator obtained with  $n_{EOT} = 2.84 \times 10^{11}$  100 GeV electrons on target (EOT) [48–50]. If the  $\varphi$  exists, it could be produced in the reaction

$$eZ \rightarrow \mu Z \varphi; \varphi \rightarrow invisible \quad (22)$$

of high-energy electrons scattering off nuclei of an active target of a hermetic NA64e detector, followed by the prompt invisible  $\varphi$  decay into DM particles, which carry away part of the beam energy. A more detailed description of the NA64e detector can be found in Refs.[49, 50]. Below, its main relevant features will be briefly mentioned. The detector schematically shown in Fig.2 employed a 100 GeV pure electron beam, using the H4 beam-line of the CERN's North Area with intensity of up to  $\simeq 10^7$  electrons per spill. The beam electrons impinging the target are measured by a magnetic spectrometer consisting of two successive dipole magnets and a low-material-budget tracker chambers  $T1 - T4$  [51]. The beam electrons are tagged by detecting the synchrotron radiation (SR) emitted by them in the magnets with the SRD counter [52]. The active target is an electromagnetic calorimeter (ECAL), followed by a hermetic hadronic calorimeter (HCAL) consisting of three consecutive modules. The HCAL and the counters MU1-MU3, located between the modules, are used as an efficient veto against hadronic secondaries and also for identification of muons produced in the primary  $e^-$  interactions in the final state.

The signature of the reaction (22) would be an event with a fraction of the beam energy deposited in the ECAL accompanied by a single muon outgoing from the target and passing the three HCAL modules, as shown in Fig.2. In these searches a sample of  $\simeq 10^4$  rare dimuon events from the QED production in the target, dominated by the hard bremsstrahlung photon conversion into the  $\mu^+\mu^-$  pair on a target nucleus,  $e^-Z \rightarrow e^-Z\gamma; \gamma \rightarrow \mu^+\mu^-$  was accumulated. Differently from the reaction (22) shown in Fig.2, these events are accompanied by two muons in the final state passing through the HCAL modules. They exhibit themselves as a narrow strip in the measured distribution of events in the  $(E_{ECAL}; E_{HCAL})$  plane corresponding to the double MIP (minimum ionizing particle) HCAL energy  $E_{HCAL} \simeq 12$  GeV [49, 50], see, e.g. Fig. 2 (left panel) in Ref.[50] (region I). Using these samples we define the signal region for events from (22) to be  $(E_{ECAL} < 50$  GeV;  $E_{HCAL} \simeq 6$  GeV) where the first cut is on the missing energy in the ECAL carried away

by the  $\varphi$  and the muon, also used in Ref. [50] for the search for invisible decays of  $A'$ 's [49, 50]); while the second requirement is for the total energy in three HCAL modules to be equal the MIP energy deposited by a single muon.

Interestingly, several events are observed in the signal region, the origin of which is the subject of further detailed analysis beyond the scope of this work. Conservatively attributing these events to background, we estimated the NA64e sensitivity with a generic DM simulation package DMG4 [53] used for the signal yield, the efficiency of the signal muon detection and detector acceptance calculations, e.g., as in Ref.[54].

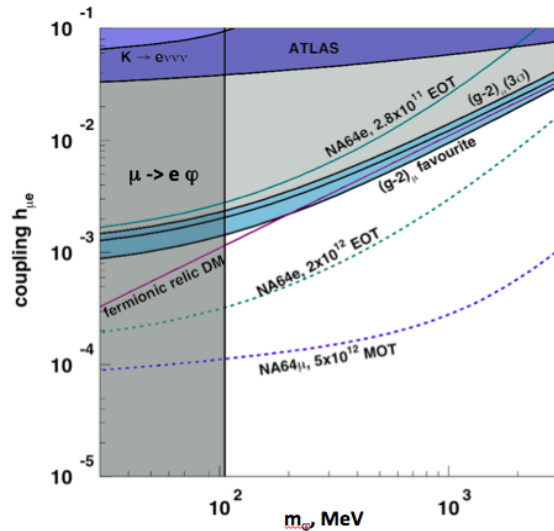


FIG. 3: The current constraints on the coupling  $h_{\mu e}$  in the  $(m_\varphi, h_{\mu e})$  plane (dark dashed area) from the  $\mu \rightarrow e\varphi$  [37],  $K \rightarrow e\nu\nu$  decays [47], the ATLAS experiment [46], and  $(g-2)_\mu$  anomaly ( $3\sigma$  level). The 90% C.L. exclusion regions from NA64e with  $\simeq 2.8 \times 10^{11}$  EOT and projection from NA64e with  $\simeq 2 \times 10^{12}$  EOT and NA64 $\mu$  with  $\simeq 5 \times 10^{12}$  MOT [17, 19] are also shown (areas above dashed curves). The  $(g-2)_\mu$  favored parameter region (dashed blue area) and the curve explaining the DM relic abundance for fermionic case calculated with  $g_{\varphi\psi_1\psi_2} = 0.08$  assuming  $\frac{m_\psi}{m_\varphi} = \frac{1}{3}$  are also shown.

The combined 90% C.L. exclusion limits on the coupling parameter  $h_{\mu e}$  as a function of the  $\varphi$  mass are shown in Fig. 3. For the region  $m_\varphi \lesssim 0.5$  GeV, NA64 bounds are more stringent than those derived from the  $(g-2)_\mu$  and ATLAS experiment, excluding part of the parameter space favored by the muon anomaly.

For further searches, NA64e is planned to be upgraded with a magnetic spectrometer downstream the HCAL for the measuring of both, the outgoing muon momentum and, in combination with the ECAL, the missing energy carried away by the  $\varphi$ , thus allowing significantly improve the search sensitivity.

Another complementary search could be performed with the NA64 $\mu$  experiment at M2 muon beam of the

CERN SPS [17, 19] by using the  $\varphi$  production in the inverse reaction

$$\mu Z \rightarrow eZ\varphi; \varphi \rightarrow \textit{invisible} \quad (23)$$

of 100-160 GeV muon scattering on heavy nuclei. The projection sensitivity for the  $\varphi$  searches with reactions (22) and (23) is shown in Fig.3 for the background-free case. One can see that with the statistics increased by an order of magnitude one can decisively probe the parameter space explaining the  $(g-2)_\mu$  and the current density of dark matter. The  $(m_\varphi, h_{\mu e})$  region of interest could also be effectively tested with the planned M<sup>3</sup>[23] and LDMX [55–57] experiments by using the missing mo-

mentum technique.

Finally, note that the model additionally predicts contribution to the anomalous electron magnetic moment at the level  $\Delta a_e = 0.6 \times 10^{-13}$ . This value is a factor five less than the current error on  $\Delta a_e = (4.8 \pm 3.0) \times 10^{-13}$  determined from the recent precise measurements of the fine-structure constant [58], and hopefully can be probed in the near future.

We are grateful to our colleagues from the NA64 Collaboration for their interest, useful discussions, and valuable comments. We would also like to thank A.N. Toropin for his help in handling the data sample and D.V. Kirpichnikov for the discussion on limit calculations.

- 
- [1] B. Abi *et al.*, Phys. Rev. Lett. **126**, 141801 (2021)
- [2] G.W. Bennett *et al.*, Phys. Rev. D **43**, 072003 (2006).
- [3] T. Aoyama *et al.*, Phys. Rep. **887**, 1 (2020).
- [4] T. Aoyama, M. Hayakawa, T. Kinoshita, and M. Nio, Phys. Rev. Lett. **109**, 111808 (2012).
- [5] K. Melnikov and A. Vainshtein, Phys. Rev. D **70**, 113006 (2004).
- [6] A. Czarnecki, W. J. Marciano, and A. Vainshtein, Phys. Rev. D **67**, 073006 (2003); [erratum: Phys. Rev. D **73**, 119901 (2006)].
- [7] A. Kurz, T. Liu, P. Marquard, and M. Steinhauser, Phys. Lett. B **734**, 144 (2014).
- [8] M. Hoferichter, B. L. Hoid, B. Kubis, S. Leupold, and S. P. Schneider, JHEP **10**, 141 (2018).
- [9] A. Keshavarzi, D. Nomura, and T. Teubner, Phys. Rev. D **97**, 114025 (2018); Phys. Rev. D **101**, 014029 (2020).
- [10] G. Colangelo, M. Hoferichter, and P. Stoffer, JHEP **02**, 006 (2019).
- [11] M. Hoferichter, B. L. Hoid, and B. Kubis, JHEP **08**, 137 (2019).
- [12] A. Gerardin, H. B. Meyer, and A. Nyffeler, Phys. Rev. D **100**, 034520 (2019).
- [13] M. Davier, A. Hoecker, B. Malaescu, and Z. Zhang, Eur. Phys. J. C **80**, 241 (2020); [erratum: Eur. Phys. J. C **80**, 410 (2020)].
- [14] T. Blum, N. Christ, M. Hayakawa, T. Izubuchi, L. Jin, C. Jung, and C. Lehner, Phys. Rev. Lett. **124**, 132002 (2020).
- [15] P. Athron, C. Balázs, D.H. Jacob, W. Kotlarski, D. Stöckinger and H. Stöckinger-Kim, JHEP **09**, 080 (2021).
- [16] S. N. Gninenko and N. V. Krasnikov, Phys. Lett. B **513**, 119 (2001).
- [17] S. N. Gninenko, N. V. Krasnikov, and V. A. Matveev, Phys. Rev. D **91**, 095015 (2015).
- [18] S. N. Gninenko and N. V. Krasnikov, Phys. Lett. B **783**, 24 (2018).
- [19] H. Sieber, D. Banerjee, P. Crivelli, E. Depero, S. N. Gninenko, D. V. Kirpichnikov, M. M. Kirsanov, V. Poliakov, and L. Molina Bueno, Phys. Rev. D. **105**, 052006 (2022).
- [20] D. V. Kirpichnikov, H. Sieber, L. Molina Bueno, P. Crivelli, and M. M. Kirsanov, Phys. Rev. D **104**, 076012 (2021).
- [21] D. V. Kirpichnikov, V. E. Lyubovitskij, and A. S. Zhevlakov, Phys. Rev. D **102**, 095024 (2020).
- [22] C. Cazzaniga *et al.* (NA64 Collaboration), Eur. Phys. J. C **81**, 959 (2021).
- [23] Y. Kahn, G. Krnjaic, N. Tran, and A. Whitbeck, JHEP **09**, 153 (2018).
- [24] I. Holst, D. Hooper, and G. Krnjaic, Phys. Rev. Lett. **128**, 141802 (2022).
- [25] R. Capdevilla, D. Curtin, Y. Kahn, and G. Krnjaic, arXiv:2112.08377.
- [26] Chien-Yi Chen, M. Pospelov, and Yi-Ming Zhong, Phys. Rev. D **95**, 115005 (2017).
- [27] J. Jaeckel and A. Ringwald, Annu. Rev. Nucl. Part. Sci. **60**, 405 (2010).
- [28] R. Essig *et al.*, arXiv:1311.0029.
- [29] J. Alexander *et al.*, arXiv:1608.08632.
- [30] M. Battaglieri *et al.*, arXiv:1707.04591.
- [31] J. Beacham *et al.*, J. Phys. G **47**, 010501 (2020); arXiv:1901.09966.
- [32] H. Davvoudiasl and W.J. Marciano, Phys. Rev. D **98**, 075011 (2018).
- [33] C. Y. Chen, H. Davvoudiasl, W. J. Marciano, and C. Zhang, Phys. Rev. D **93**, 035006 (2016).
- [34] B. Batell, N. Lange, D. McKeen, M. Pospelov, and A. Ritz, Phys. Rev. D **95**, 075003 (2017).
- [35] S.N. Gninenko and N.V. Krasnikov, EPJ Web Conf. **125**, 02001 (2016).
- [36] S.N. Gninenko and N.V. Krasnikov, Mod. Phys. Lett. A **31**, 1650142 (2016).
- [37] P. A. Zyla *et al.* (Particle Data Group), Prog. Theor. Exp. Phys. **2020**, 083C01 (2020).
- [38] As a review, see for example, F. Jegerlehner and A. Nyffeler, Phys. Rep. **477** 1 (2009).
- [39] P.A.R. Ade *et al.* (Planck Collaboration), Astron. Astrophys. A **13** 594 (2016).
- [40] E.W. Kolb and M. S. Turner, Front. Phys. **69** 1 (1990).
- [41] D.S. Gorbunov and V.A. Rubakov, *Introduction to the theory of the early Universe* (World Scientific Publishing Co. Pt. Ltd., Singapore, 2011).
- [42] P. Gondolo and G. Gelmini, Nucl. Phys. **B360** 145 (1991).
- [43] S. N. Gninenko, N. V. Krasnikov, and V. A. Matveev, Phys. Part. Nucl. **51** 829 (2020).
- [44] S. N. Gninenko, N. V. Krasnikov, and V. A. Matveev, Usp. Fiz. Nauk **191** 1361 (2021).
- [45] S. Profumo, arXiv:1301.0952.

- [46] G. Aad *et al.* (ATLAS Collaboration), Phys. Rev. D **90**, 072010 (2014).
- [47] J. Heintze *et al.*, Nucl. Phys. **B149**, 365 (1979).
- [48] D. Banerjee *et al.* (NA64 Collaboration), Phys. Rev. Lett. **118**, 011802 (2017).
- [49] D. Banerjee *et al.* (NA64 Collaboration), Phys. Rev. D **97**, 072002 (2018).
- [50] D. Banerjee *et al.* (NA64 Collaboration), Phys. Rev. Lett. **123**, 121801 (2019).
- [51] D. Banerjee, P. Crivelli, and A. Rubbia, Adv. High Energy Phys. **2015**, 105730 (2015).
- [52] E. Depero *et al.*, Nucl. Instrum. Methods Phys. Res., Sect. A **866**, 196 (2017).
- [53] A. Celentano, M. Bondi, R. R. Dusaev, D. V. Kirpichnikov, M. M. Kirsanov, N. V. Krasnikov, L. Marsicano, and D. Shchukin, Comput. Phys. Commun. **269**, 108129 (2021).
- [54] Yu.M.. Andreev *et al.* (NA64 Collaboration), Phys. Rev. Lett. **126**, 211802 (2021).
- [55] T. Akesson *et al.* (LDMX Collaboration), arXiv:1808.05219.
- [56] T. Akesson *et al.* (LDMX Collaboration), JHEP **04**, 003 (2020).
- [57] A. Berlin, N. Blinov, G. Krnjaic, P. Schuster, and N. Toro, Phys. Rev. D **99**, 075001 (2019).
- [58] L. Morel, Zh. Yao, P. Cladé, and S. Guellati-Khélifa, Nature (London) **588**, 61 (2020).
- [59]  $p_{ecm} = \sqrt{E_{ecm}^2 - m_e^2}$ ,  $E_{ecm} = \frac{s+m_e^2-m_\mu^2}{2\sqrt{s}}$ ,  $s = (m_1+m_2)^2$ .
- [60] For  $m_2 > m_1 + m_e + m_\mu$  the heaviest DM particle  $s_2$  is unstable and it decays into the lightest DM particle  $s_1$  and  $\mu e$  pair, namely  $s_2 \rightarrow s_1^* \mu^- e^+$  that in full analogy with the case of pseudo Dirac light matter allows us to escape Planck restrictions.